

An Unstable Structured Liquid: Film Thickness Dependence of the Early Stage Evolution

Ratchana Limary[‡] and Peter F. Green^{*,†,‡}

Department of Chemical Engineering and Texas Materials Institute, Graduate Program in Materials Science and Engineering, The University of Texas at Austin, Austin, Texas 78712

Received February 22, 2002

Revised Manuscript Received May 20, 2002

Bulk symmetric A–B diblock copolymers undergo a transition from an isotropic to an alternating lamellar phase, characterized by period L , below an order–disorder transition (ODT) temperature. The ODT is defined by $\chi N = 10.5$, where N is the degree of polymerization of the chain and χ is the Flory–Huggins interaction parameter.¹ In thin films the long-range order and orientation of the lamellae, as well as the ODT, are influenced by confinement effects and by interfacial interactions.^{2–11} When either the A or B component is preferentially attracted to the polymer/air (vacuum) interface or to the polymer/substrate interface, the lamellae align parallel to the interfaces. An asymmetric wetting situation arises when a different block is attracted to each interface. Experiments on copolymer films with $\chi N > 10.5$ reveal that the layer in contact with the substrate is of thickness $L/2$, whereas subsequent layers are of thickness L , provided that the film is sufficiently thick. The topography of the film is determined by the commensurability between the film thickness, h , and L . When $h = (n + 1/2)L$, the layer in contact with the free surface is uniform in thickness (i.e., smooth outer surface) whereas it is discontinuous, comprising islands, holes, or interconnected patterns when $h \neq (n + 1/2)L$.^{2,3,7}

Diblock copolymer thin films above the bulk ODT, in contrast, may exhibit properties that are similar to simple homopolymer liquids yet, at the same time, retain properties akin to block copolymers.^{2,8} We recently showed that symmetric polystyrene-*b*-poly(methyl methacrylate) (PS-*b*-PMMA) diblock copolymers of $\chi N = 7.5$ exhibited transient and stable topographies on SiO_x/Si substrates, depending on the film thickness.⁸ Films of initial thickness $h < 3.5$ nm spontaneously formed spinodal patterns, whereas holes developed throughout films in the thickness range $3.5 \text{ nm} < h < 7$ nm. On the other hand, the topographies of films in the thickness range $9.5 \text{ nm} < h < 15$ nm exhibited transient spinodal patterns and subsequently formed droplets on an underlying layer (“brush”) of thickness $h_L = 7$ nm, anchored to the substrate. The thickness of this anchored layer is $L/2$, and its existence is associated with order induced into the film due to interactions with the substrate.^{9–12} Further, we showed that holes developed throughout the surfaces of films in the thickness range $20 \text{ nm} < h < 35$ nm. All the topographies that developed in films in the thickness range $7 \text{ nm} < h < 35$ nm eventually formed droplets on the “brush” layer.

For thicknesses $h > 35$ nm, the films were stable, with smooth surfaces.

In this paper we are specifically interested in the *early stage* time dependence and film thickness dependence of the structural evolution of the topographies of thin films of this PS-*b*-PMMA diblock copolymer ($\chi N = 7.5$, $9 \text{ nm} < h < 18 \text{ nm}$) on SiO_x/Si substrates. We show that local thickness fluctuations which occur during the *early stage* of structural evolution (linear *amplification* regime) of films in the thickness range $9.5 \text{ nm} < h < 15$ nm are characterized by a dominant wave vector, q . The q vector remains relatively constant, independent of time, during this stage. Simultaneously, the amplitude of the thickness fluctuations, δh , increased in a manner consistent with an exponential. Moreover, the q vector and the relaxation, or rise time, τ , associated with the growth of the instability, exhibit relatively weak film thickness dependencies. In contrast, instabilities in thin *homogeneous* films driven purely by van der Waals, dispersive, interactions lead to strong film thickness dependencies $q \sim h^{-2}$ and to $\tau \sim h^{5.14-19}$.

Thin films of a symmetric poly(styrene-*b*-methyl methyl acrylate) (PS-*b*-PMMA) diblock copolymer ($\chi N = 7.5$, $N = N_{\text{PS}} + N_{\text{PMMA}} = 201$; $f \sim 0.5$, polydispersity index $M_w/M_n = 1.14$) were prepared in SiO_x/Si substrates. Films that ranged in thickness from $h = 9.5$ nm to 19.5 nm were examined. AFM indicates that the as-cast films were flat and smooth, exhibiting no topographical features. The samples were subsequently annealed at 170°C under vacuum ($\sim 10^{-5}$ Torr) conditions. The glass transition temperatures of the homopolymer components of the diblocks are 100°C for PS and 115°C for PMMA. Samples were periodically quenched to room temperature, and topographical analyses of the same regions of the films were performed each time. We reiterate that for all films a layer of copolymer of thickness $h_d = (h - h_L)$, where $h_L = 7$ nm, became unstable and eventually formed droplets on an underlying layer of polymer of thickness $h_L = 7$ nm anchored to the SiO_x layer.

During the early stage of pattern evolution, the topography of each sample roughened. The spatial periodicity of the fluctuations at a given instant are characterized by a dominant wave vector, q , obtained from fast Fourier transforms (FFT) of AFM images of the topographies. AFM profiles of the topographies also provided information about the average amplitude of the thickness fluctuations, δh , of each sample. We analyzed images which ranged in size from 20×20 to $80 \times 80 \mu\text{m}^2$. Figure 1 shows a $50 \times 50 \mu\text{m}^2$ image of a spinodal pattern on the $h_{\text{min}} = 7$ nm “brush” at time $t = 44$ min for a film of $h = 11.5$ nm. The circular ring, the fast Fourier transform of the image in this figure, is typical of the samples we examined. The circularity indicates that the features in the scan are isotropic. For this sample, the average breakup time ($\delta h = h_d$) occurred at $t_b = 18$ min. Hence, the image in Figure 1 represents the topography of the film after rupturing.

We begin by discussing results from samples in the thickness range $9.5 \text{ nm} < h < 15$ nm. While during the early (amplification) stage the q vector exhibited a weak, nearly constant, dependence on time, the average amplitude of the local variations in height, δh , increased in a manner consistent with an exponential. The time

[†] Department of Chemical Engineering and Texas Materials Institute.

[‡] Graduate Program in Materials Science and Engineering.

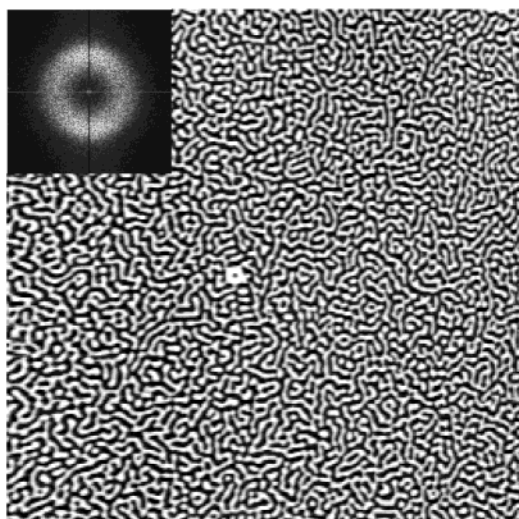


Figure 1. A ($50 \times 50 \mu\text{m}^2$) two-dimensional image of the spinodal-like pattern. This sample of initial thickness $h = 11.5$ nm was annealed for a time $t = 44$ min, just larger than t_b . A FFT, from which the q vector was determined, is shown in the inset.

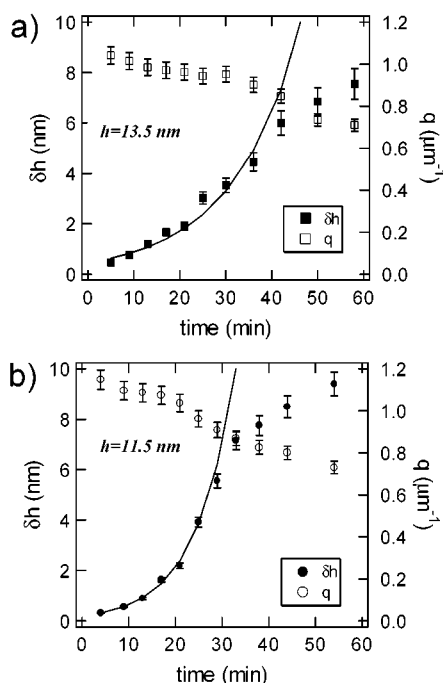


Figure 2. Time dependencies of δh and of the wave vector q for films of two different thicknesses: (a) 13.5 nm and (b) 11.5 nm. During the early stage of pattern evolution ($t < 30$ min for the thicker film and $t < 20$ min for the thinner film), q is relatively insensitive to time while δh increases exponentially with time.

dependencies of the wave vector, q , and of the evolution of the average height of the fluctuations δh are shown in Figure 2 for samples of thickness $h = 13.5$ nm (a) and $h = 11.5$ nm (b). Note that at longer times the q vector decreased more rapidly with time while the rate of growth of δh decreased. It is noteworthy that this decrease in the q vector with time is not associated with coarsening of the structure since coarsening would occur only for $t > t_b$. The time $t = t_b$ is identified as the average time at which the film ruptured on a macroscopic scale. The time $t_b = 50$ min for the $h = 13.5$ nm film and, as mentioned earlier, $t_b = 18$ min for the $h = 11.5$ nm film. This decrease in the q vector simply reflects a transition

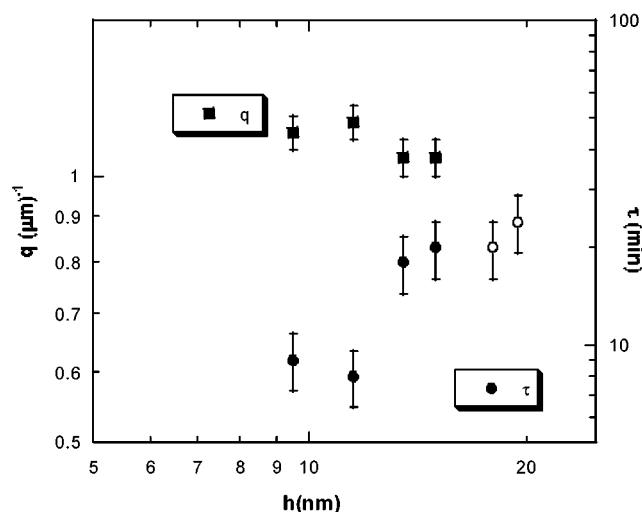


Figure 3. Film thickness dependencies of the q vector and the rise time, or equivalently the relaxation time, τ , during the early stage of structural evolution. The lines drawn through the data are guides to the eye.

beyond the so-called linear regime when δh became sufficiently large.

The q vector and the relaxation time associated with the growth of δh are plotted as a function of film thickness in Figure 3 for the early, so-called, linear stage. These data show that τ increases with h ($h = 15$ nm). In this thickness range, the q vector exhibits only a very weak variation with h . Below we discuss these observations regarding the time and film thickness dependencies of q and the thickness dependence of τ .

It is known that the existence of surface instabilities may be understood in terms of the dependence of an effective interfacial free energy, ΔF_{copl} , on film thickness.¹¹ ΔF_{copl} is the difference between the free energy of a thick film and that of a thin film of thickness h . Shall calculated ΔF_{copl} for block copolymer films of varying thickness for a wide range of values of χN , above and below the ODT, and for different wetting conditions.⁹ The $\Delta F_{\text{copl}}/k_B T$ vs h curve for our PS-*b*-PMMA diblock ($\chi N = 7.5$) is shown in Figure 4 for a sample on a substrate that preferentially attracts the PMMA block component while the PS component is attracted to the free surface. The existence of the underlying brush layer of $h_L = 7$ nm is associated with the location of minimum in the ΔF_{copl} vs h plot. The value of h_L is equal to one-half of the lamellar thickness, $L/2$.^{2,8,11}

Typically, the existence of spinodal patterns in very thin liquid films is generally associated with an interfacial free energy, ΔF_{vdf} , determined by destabilizing long-range (dispersive) van der Waals intermolecular interactions,^{13–19} where

$$\Delta F_{\text{vdf}}(h) = -\frac{A_{\text{s/f/a}}}{12\pi h^2} \quad (1)$$

In this equation, $A_{\text{s/f/a}}$ is an effective Hamaker constant expressed in terms of the individual Hamaker constants of the system: the substrate, the film, and the surrounding medium. When $A_{\text{s/f/a}} > 0$, there is a net attraction between the film/air and film/substrate interfaces, the effect of which is to thin the film locally. Films in the thickness range where the curvature of free energy vs film thickness dependence is negative, $\partial^2 \Delta F_{\text{vdf}} / \partial h^2 < 0$, are unstable and form spinodal patterns. In

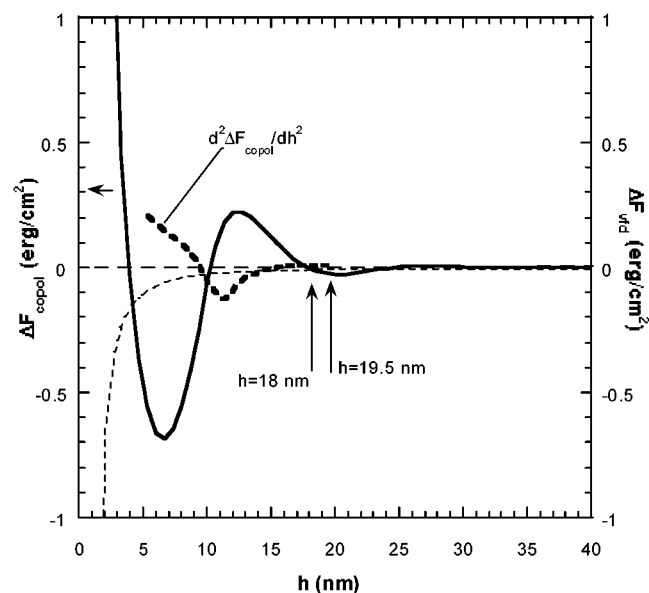


Figure 4. (a) A sketch of effective interfacial free energy as a function of film thickness for a symmetric block copolymer with $\chi N = 7.5$, $R_g = 3.5$ nm, and $V = 33$ nm³ for the asymmetric wetting case examined here. The $\partial^2 \Delta F_{\text{copol}} / \partial h^2$ curve is identified in the figure. The data used to plot this curve were calculated from the ΔF_{copol} data using a finite difference method. The dispersive contributions to the free energy (eq 2), assuming $A_{\text{sf}} = 10^{-19}$ J, are plotted as a function of film thickness. The value of A that we used is comparable to values of PS on SiO₂/Si. Note that they not important for $h > L/2$.

our system the curvature of our interfacial free energy function, $\partial^2 \Delta F_{\text{copol}} / \partial h^2$, is negative in the range $9.5 \text{ nm} \leq h \leq 15 \text{ nm}$, as shown in Figure 4. The negative curvature of the free energy is, of course, responsible for the existence of the "spinodal" patterns in this system and is associated with the connectivity of the blocks.

Small-amplitude fluctuations at the surface will become amplified by the disjoining pressure ($\propto \partial^2 \Delta F_{\text{vfd}} / \partial h^2$). The amplitude, δh , of the fluctuations due to pressure gradients is predicted to increase exponentially in the linear regime, characterized by a relaxation time, τ ¹⁸

$$\delta h = \delta h_0 e^{t/\tau} \quad (2)$$

While the data in Figure 2 representing the time dependence of δh are consistent with an exponential, it important to realize that such an exponential growth of δh due to a linear instability is not unexpected. On the other hand, significant differences are to be expected in the film thickness dependencies of τ and q which characterize the structural evolution of the pattern.

For an instability characterized by an effective interfacial free energy of ΔF , the dominant q vector is $q \propto (h^{-2} \Delta F / \partial h^2)^{1/2}$. If the interactions are assumed to be purely van der Waals, then $q \propto h^{-2}$, and the relaxation time associated with most rapid growth is $\tau \sim h^5$. Our data (Figure 3) show much weaker film thickness dependencies for q and τ . This suggests that van der Waals forces are not responsible for the instability. This conclusion is corroborated by the results in Figure 4 which show that contributions for van der Waals interactions are negligible for the film thicknesses used in our experiments, $h > 9 \text{ nm}$.

We now comment further on the film thickness dependence of the q vector. The film thickness dependence of the q vector in our system should vary as $q \propto (-\partial^2 \Delta F_{\text{copol}} / \partial h^2)^{1/2}$ which is not a monotonic function of h . The film thickness dependence of the q vector in our experiments does not follow the above prediction for the following reason. The calculation of ΔF_{copol} assumes that the system is at equilibrium initially, with alternating A-rich and B-rich phases. It turns out that the chains in the as-cast film are in a nonequilibrium phase-mixed state. When the sample is brought to 170 °C, the chains undergo rapid phase separation during the onset of the instability. This might be expected to affect the magnitude of the q vector during the early stage.

The experiments on the samples of $h > 15 \text{ nm}$ are now discussed. While the process that characterizes the instability in films in the thickness range $9.5 \text{ nm} < h < 15 \text{ nm}$ should be spinodal, the data obtained for the $h = 19.5 \text{ nm}$ film are not. For thicknesses $15 \text{ nm} < h < 20 \text{ nm}$, $\partial^2 \Delta F_{\text{copol}} / \partial h^2$ is slightly positive and relatively constant. A large number of holes initially appear throughout these films. These holes first impinged on the substrate and then grow slightly before forming the interconnected structure that appears to be spinodal. This process is therefore a nucleation and growth process.²⁰ Moreover, we know that while at early times δh increased in a manner consistent with an exponential function the q vector decreased rapidly in comparison to the relatively constant value observed in Figure 2 for films in the thickness range $9.5 \text{ nm} < h < 15 \text{ nm}$. In ref 8 we had originally identified the points at $h = 18$ and 19.5 nm as spinodal. Clearly, knowledge of the time-dependent structural evolution is necessary to discern the difference between a nucleation and growth process and a spinodal process, particularly in a transition regime. We note that the growth stage of the nucleation and growth mechanism is very apparent in thicker films.

In conclusion, we examined the formation and evolution of spinodal patterns in structured fluid, block copolymer, thin films above the bulk ODT. The effective interfacial free energy, ΔF_{copol} , of a block copolymer thin film is known to be a periodic function of film thickness. Films with thicknesses in the regimes where ΔF_{copol} exhibits negative curvature are structurally unstable and form spinodal patterns that eventually become droplets. We showed that during the early (linear) amplification regime q and δh have similar time dependences to systems that become unstable due to van der Waals interactions, $q = \text{constant}$ and $\delta h \sim \exp(t/\tau)$. In contrast, the q vector and τ exhibit considerably weaker dependencies on h . This behavior is not unexpected on the basis of the difference between the effective interfacial free energies that control each instability.

Acknowledgment. This work was supported by the Robert A. Welch Foundation and the National Science Foundation (DMR-0072809). Discussions with Venkat Ganesan and Ken R. Shull are gratefully acknowledged.

References and Notes

- (1) Bates, F. S.; Fredrickson, G. H. *Annu. Rev. Phys. Chem.* **1990**, *41*, 525.
- (2) Green, P. F.; Limary, R. *Adv. Colloid Interface Sci.* **2001**, *94*, 53.
- (3) Fasolka, M. J.; Mayes, A. M. *Annu. Rev. Mater. Res.* **2001**, *31*, 323.

- (4) Coulon, C.; Russell, T. P.; Deline, V. R.; Green, P. F. *Macromolecules* **1989**, *22*, 2581.
- (5) Mansky, P.; Liu, Y.; Huang, E.; Russell, T. P. *Science* **1997**, *275*, 1458.
- (6) Huang, E.; Russell, T. P.; Harrison, C.; Chaikan, P. M.; Register, R. A.; Hawker, C. J.; Mays, J. *Macromolecules* **1998**, *31*, 7641.
- (7) Russell, T. P. *Curr. Opin. Colloid Interface Sci.* **1996**, *1*, 107.
- (8) Limary, R.; Green, P. F. *Macromolecules* **1999**, *32*, 8167.
- (9) Shull, K. R. *Macromolecules* **1992**, *25*, 2122.
- (10) Fredrickson, G. H. *Macromolecules* **1987**, *20*, 2535.
- (11) Limary, R.; Green, P. F.; Shull, K. R. *Eur. Phys. J.: E*, in press.
- (12) Masson, J.-L.; Limary, R.; Green, P. F. *J. Chem. Phys.* **2001**, *114*, 10963.
- (13) Seeman, R.; Herminghaus, S.; Jacobs, K. *Phys. Rev. Lett.* **2001**, *86*, 5534.
- (14) Xie, R.; Karim, A.; Douglas, J. F.; Han, C. C.; Weiss, R. A. *Phys. Rev. Lett.* **1998**, *81*, 1251.
- (15) Sharma, A.; Khanna, R. *Phys. Rev. Lett.* **1998**, *81*, 3463.
- (16) Vrij, A.; Overbeek, J. T. G. *J. Am. Chem. Soc.* **1968**, *90*, 3074.
- (17) Brochard Wyart, F.; Daillant, J. *Can. J. Phys.* **1990**, *68*, 1084.
- (18) *Interfacial Transport Processes and Rheology*; Edwards, D. A., Brenner, H., Wasan, D. T., Eds.; Butterworth Series in Chemical Engineering; Butterworth: New York, 1991.
- (19) Reiter, G.; Khanna, R.; Sharma, A. *Phys. Rev. Lett.* **85**, 1432.
- (20) Khanna, R.; Sharma, A.; Reiter, G. *EPJ Direct* **2000**, *E2*, 1.

MA025509O